Applied Physics Letters

Evidence for carbon clusters present near thermal gate oxides affecting the electronic band structure in SiC-MOSFET

Cite as: Appl. Phys. Lett. **115**, 101601 (2019); https://doi.org/10.1063/1.5112779
Submitted: 03 June 2019 . Accepted: 03 August 2019 . Published Online: 06 September 2019

D. Dutta, D. S. De, D. Fan, S. Roy, G. Alfieri, M. Camarda, M. Amsler, J. Lehmann, H. Bartolf, S. Goedecker, and T. A. Jung

Applied Physics Letters ARTICLE scitation.org/journal/apl

Evidence for carbon clusters present near thermal gate oxides affecting the electronic band structure in SiC-MOSFET

Cite as: Appl. Phys. Lett. **115**, 101601 (2019); doi: 10.1063/1.5112779
Submitted: 3 June 2019 · Accepted: 3 August 2019 ·
Published Online: 6 September 2019

View Online Export Citation CrossMark

D. Dutta,[1,a] D. S. De,[2] D. Fan,[1] S. Roy,[2] G. Alfieri,[3] M. Camarda,[1] M. Amsler,[4] J. Lehmann,[3] H. Bartolf,[3,b] S. Goedecker,[2,a] and T. A. Jung[1,a]

AFFILIATIONS

[1]Laboratory for Micro and Nanotechnology, Paul Scherrer Institute, CH-5232 Villigen PSI, Switzerland
[2]Departement of Physics, University of Basel, CH-4056 Basel, Switzerland
[3]ABB Switzerland Ltd., Corporate Research, CH-5405 Baden-Dättwil, Switzerland
[4]Laboratory of Atomic and Solid State Physics, Cornell University, Ithaca, New York 14853, USA

[a]**Authors to whom correspondence should be addressed:** dipanwita.dutta@psi.ch, stefan.goedecker@unibas.ch, and thomas.jung@psi.ch
[b]**Present address:** Robert Bosch GmbH, Automotive Electronics, D-72762 Reutlingen, Germany.

ABSTRACT

High power SiC MOSFET technologies are critical for energy saving in, e.g., distribution of electrical power. They suffer, however, from low near-interface mobility, the origin of which has not yet been conclusively determined. Here, we present unique concerting evidence for the presence of interface defects in the form of carbon clusters at native thermally processed oxides of SiC. These clusters, with a diameter of 2–5 nm, are HF-etch resistant and possess a mixture of graphitic (sp2) and amorphous (sp3 mixed in sp2) carbon bonds different from the normal sp3 carbon present in 4H-SiC. The nucleation of such defects during thermal oxidation as well as their atomic structure is elucidated by state-of-the-art atomistic and electronic structure calculations. In addition, our property prediction techniques show the impact of the simulated carbon accumulates on the electronic structure at the interface.

Controlling interface architectures and dopant profiles with minimal defect densities on the nanometer scale is of eminent importance to advance semiconductor technologies,[1] in particular, to alleviate the current limitations of power semiconductors and Silicon Carbide (SiC) Metal Semiconductor Field Effect Transistor (MOSFET) devices. Planar, atomically well-defined (∼10 nm–40 nm) gate insulator layers in nanometer-close proximity (<25 nm) to defect-free semiconducting channels are required to sustain a high carrier mobility and gate-oxide reliability.[2]

SiC is the only wide-bandgap material with a native oxide (silicon dioxide, SiO_2) that can be grown using a thermal process.[3] Unfortunately, however, the thermal oxidation of SiC—in contrast to Si—curtails the channel mobility to merely below ∼40 cm^2/V s, compared to ∼900 cm^2/V s in bulk 4H-SiC crystals. Extensive efforts have been undertaken to increase the near-interface mobility, e.g., via surface conditioning or passivation of the SiC during interface fabrication.[7–9] The origin and physical nature of the structural defects and their effect as carrier traps have been the subject of intense research.[3,10,11] Defects modify the electronic properties of the inversion channel, thus deteriorating the field-effect channel mobility and introducing scattering centers for the charge carriers.[4,5] The physical origin of the near interface traps (NITs) remains unclear, but recent studies suggest the formation of carbon clusters, such as carbon dimers, or graphitic microcrystals at the interface.[6,12,13] Experimental evidence for their presence has been concluded from atomic force microscopy (AFM) studies of SiC surfaces after oxide removal.[14] In the current letter, we present unique concerting evidence for the complex thermal oxidation process of SiC causing interface defects in the form of carbon clusters. This has been achieved by combining atomic force micrographs of oxygen stripped interfaces with the Raman analysis of the near-interface carbon and by performing minima hopping Density Functional Theory simulations of the oxidation process and the near interface structures and properties.

To investigate the near-gate oxide interface region, planar metal-oxide-semiconductor (MOS) capacitors were fabricated on n-type 4H-SiC (0001) (4° off-axis with 5 μm, 7–10 × 10^{15} cm^{-3} Al-doped *p*-type epilayers were used) by thermally growing a 50 nm gate oxide in a pure oxygen atmosphere at 1150 °C for 9 h (referred to as TGO in the following). As a reference, we also investigated a MOS structure fabricated by growing a 50 nm gate oxide in a passivating N_2O atmosphere at 1250 °C for 14 h (referred to as pTGO).[17] The top layer contacts of the fabricated MOS capacitors were stripped off using a standard etching solution followed by a subsequent SiO_2 removal cycle in a 2% HF bath. The duration of this HF exposure was systematically controlled in order to analyze the effect of the progressing etch process. AFM and Raman spectroscopy were carried out on the etched samples. Vibrational spectroscopy, for the detection of C bonds in the specimens, was carried out using a home-built micro Raman spectroscopy setup based on a 532 nm single mode continuous wave laser.

Additionally, structure prediction was performed by the Minima Hopping method (MHM)[15,16] at the density functional tight binding (DFTB) level. The MHM simulations were performed using the MINHOCAO package based on the DFTB[26–28] scheme to evaluate the potential energy landscape. The density functional theory (DFT) calculations were performed within the projector augmented wave framework as implemented in the VASP package[36] to refine the geometries and energetic ranking of the most promising candidate structures. The generalized gradient approximation was used with the Perdew-Burke-Ernzerhof parametrization of the exchange-correlation functional.[28,29] The bandgap of 4H-SiC, calculated using the HSE06 hybrid functional,[30] is comparable with the experimental value of 3.3 eV.[11,30]

In the top three panels of Fig. 1, we show the MOS capacitor interfaces using room temperature AFM, thereby exposing the misoriented, 4° off (0001) Si face.[18] AFM was used in the tapping mode to assess the morphology of the specimens at different stages of the HF etching process. For both samples, TGO and pTGO, we observe terraces and step bunch areas on SiC in the AFM images, which can be attributed to regions with different surface/interface energies.[19] The quasiperiodic step like structure is interesting as it looks similar to the surface morphology after step-flow[20] like growth processes,[21] but occurs here below the surface, at the oxide/SiC interface.[31] The AFM data reveals height differences across the step bunches in the range of ∼1.5–3.5 nm down to single step heights of ∼0.75 nm close to the size of one 4H-SiC unit cell (4 bilayers along the 001 direction).[22] Besides these common structural features, the most striking characteristics of the oxide stripped interfaces of TGO are the clearly observable clusters (size ∼2–∼6 nm) arranged like chains of knots of different sizes in Fig. 1(a). These are especially apparent in the AFM images after the first oxide removal and cleaning cycle (2 min, 2% HF) and are frequently, but not exclusively, located near the step bunches. After a second cycle of HF cleaning, the number of these clusters declines drastically [Fig. 1(b)]. This can be a result due to a longer exposure of the slower oxidizing agent HF in H_20, which takes a longer time to remove the carbon. In contrast to the TGO samples, pTGO has a clean interface morphology with virtually no etch resistant clusters at the interface [Fig. 1(c)]. Interestingly, the observed lower density of morphological defects in pTGO in contrast to TGO samples is in line with the earlier reports.[23] In a further series of experiments, the observed clusters at SiC/SiO_2 interfaces resisted HF etching but could be removed by ozone, providing further evidence for the carbon content,

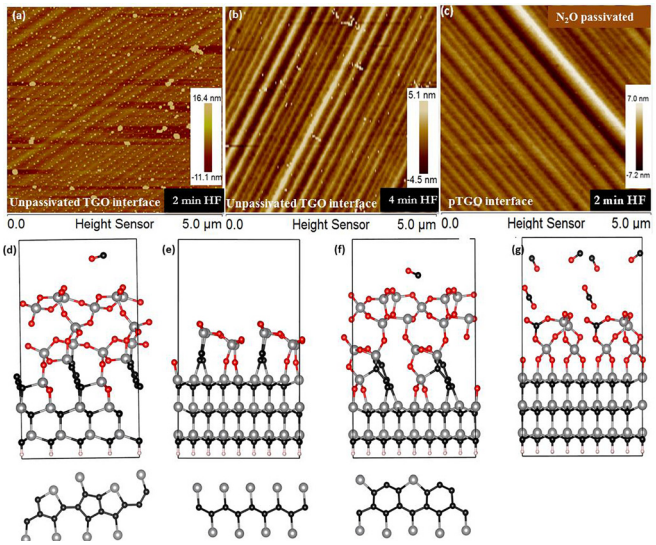

FIG. 1. Atomic Force micrographs and MHM simulations of etch resistant clusters at the SiC/SiO_2 interface after thermal oxidation: (a)–(c) AFM of the interface morphology after oxidation in pure oxygen ("TGO" sample) and in passivating N_2O ("pTGO" sample) and subsequent oxide removal using HF. (a) TGO sample after 2 min of HF etch: 2–7 nm sized etch residue line up at steps. (b) TGO sample after 4 min of HF etch: significantly fewer residues persist; (c) pTGO oxide after 2 min HF etch: virtually no clusters are detected compared to (a). (d)–(g) Numerically predicted interface structure after oxygen deficient oxidation (model B, see the main text) and subsequent oxide removal. The carbon clusters are anchored via Si to the interface (d)–(f). The clusters are HF persistent, in the simulation as well as in our AFM experiments. Characteristic examples of simulated carbon clusters: (d) carbon five ring chains; (e) Si bound carbon chains $[C\text{-}(Si\text{-}R)_2]_n$; (f) carbon six ring; and (g) absence of carbon clusters in the very initial oxidation stage.

an observation in our own findings in agreement with an earlier report[14,24] (see the supplementary material).

In order to provide a better microscopic understanding of such clusters occurring during the thermal oxidation of SiC, we performed MHM simulations using two different chemical configurations corresponding to the two distinct conditions during the oxidation process. In model A, we provide a larger amount of oxygen at the interface than required to oxidize the first surface layer, corresponding to a one-step oxidation process. In model B, we create an oxygen deficient reaction environment to mimic a two-step oxidation process. First, the surface is oxidized with half of the oxygen required to convert the topmost layer into a stoichiometric SiO_2 pattern before more oxygen is added. The results of our calculations are shown in Figs. 1(d)–1(h).

While the oxygen-excess model A promotes C mobility and results in clusters both at the interface and within the SiO_2 layer, the oxygen-deficient model B produces clusters predominantly at the interface. The latter clusters persist even if sufficient oxygen is provided in a second step. The carbon clusters exhibit similar structures in both models and consist of characteristic five (C_5) and six (C_6) membered rings. In the presence of sufficient oxygen (model A), these carbon rings form covalent bonds to the surrounding Si atoms in the SiC or SiO_2 matrix [Fig. 1(d)]. On the other hand, the oxygen-deficient model B leads initially to chainlike carbon structures, which subsequently convert in a second step to interlinked chains of carbon rings as the MHM simulation progresses [Figs. 1(d)–(f)]. These chain

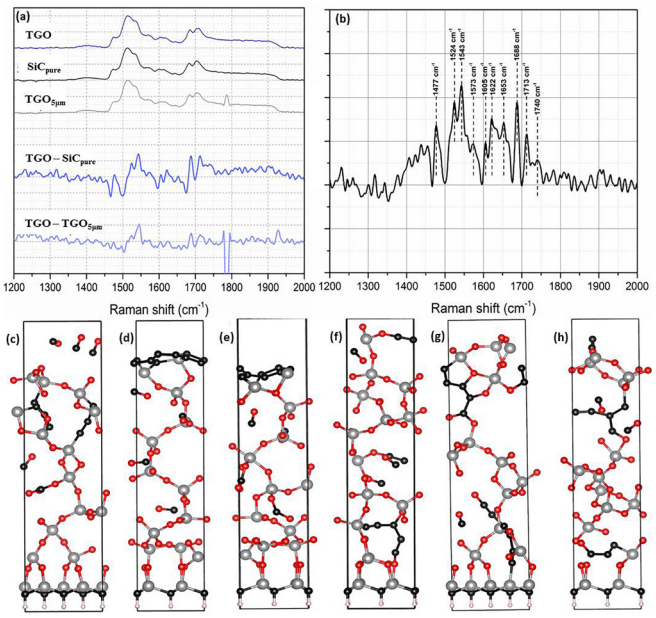

FIG. 2. Analysis of carbon bonding at the SiC/SiO_2 interface in comparison to numerically simulated structures. (a) Second order Raman spectrum of the near surface region of oxide stripped SiC/SiO_2 interfaces for TGO samples fabricated in pure oxygen. The Raman spectrum of the unprocessed "SiC_{pure}" wafer and a spectrum taken with a beam focus 5 μm below the interface ("$TGO_{5\mu m}$") have been used as reference spectra for background correction. Raman data of (TGO – $TGO_{5\mu m}$) and (TGO – SiC_{pure}) of (a); (b) Baseline corrected TGO – SiC_{pure} with the dominant graphitic peaks labeled between 1440 cm^{-1} and 1800 cm^{-1}[12–14,35] (see also Table I); (c)–(h) computed structures of the characteristic clusters obtained by an oxygen-rich in-silico process. These clusters and those shown in Figs. 1(d)–1(g) were used to simulate the Raman normal vibration modes for comparison with the experimental data in (b) (Table I). (c) Carbon nucleate in SiO_2 and (d) and (e) carbon clusters formed on the surface. (f)–(h) carbon nucleate in SiO_2 as well as at the interface of SiO_2 and SiC and also at the surface of SiO_2.

structures exhibit an especially high energetic stability at specific interface sites: the periodic silicon carbide matrix anchors/passivates the chains and ribbons from the bottom, while the Si atoms from the SiO_2 layer bond from the top.

The simulated C_5 and C_6 clusters readily represent the initial stages of the nucleation and growth process, resulting in cluster formation with a certain carbon content corresponding to the HF etch resistant clusters found in our AFM morphology. Figures 1(g) and 1(h) show the C clusters formed after further oxygen was provided in the second step of model B. In this case, the clusters are not only present at the interface but also move into SiO_2 as well. In our AFM data, we observed the etch-resistant clusters predominantly at or near SiC steps. This indicates that the clusters, possibly via a dynamic equilibrium, maintain contact with the growth front of the interface as the latter moves deeper into the SiC wafer.

In order to gain more insight into the composition of these clusters, we used second order Raman spectroscopy measurements to identify the chemical bonds involved in the observed clusters (Fig. 2).[32] For SiC, the depth of focus is >10 μm[33,34] and our samples were analyzed by moving the focal point from 0 μm to +5 μm with respect to the surface. The resulting Raman spectrum [Fig. 2(a)] after the background correction with a clean SiC wafer (referred to as SiC_{pure}) is shown in Fig. 2(b) and exhibits ten sharp peaks corresponding to vibrational excitation modes of bonds associated with the different carbon species in different bonding states (Table I).[22–25,33] The peak assignments are provided in Table I. The interpretation of the experimental Raman spectra is supported by the computed frequencies of the normal vibrational modes (Table I) for all the structures we have calculated using model B, i.e., the two step reaction process, where carbon rings are formed Figs. 2(c)–2(h). Notably, a numerical calculation of the full Raman spectrum is not feasible due to the very large number of atoms. Furthermore, laser heating or quantum confinement may lead to certain shifts in the value between theory and the measured Raman peak position.

Finally, to investigate the effect of the observed "defective" carbon on the electronic band structure of the SiC/SiO_2 interface, we performed DFT calculations based on our atomistic models. Previously, density of states (DOS) calculations were performed for small carbon

TABLE I. Comparison of our experimental and theoretical Raman signals with literature values[12–14,33] and the corresponding most plausible undesired/defective carbon bonds. All our Raman data have been compared with the assignments published by Borowicz *et al.*[33].

Experimental results (cm^{-1})	Theoretical results (cm^{-1})	Literature review (cm^{-1})	Association of each peak
1477		1470	Benzene related vibrations in finite size crystals
1524	1523	1530	3 coordinated amorphous C; polyene
		1523	
1543	1530	1554	G band for the C film with a low sp3 content
1573	1554	1594/1582	G band shift of the graphitic band (1582) due to epitaxial strain for graphene on SiC
1605			Aromatic C=C stretching
1622	1622	1622	Aromatic C=C and sp2 dimers in the sp3 phase
1653		1660	G band for ta-c
1688	1686	1686	C=C or C=O
1713	1717	1712/1720	C=O stretch symmetric stretching carbonyl/Benzene related
1740		1735	Asymmetric stretching of carbonyl C=O

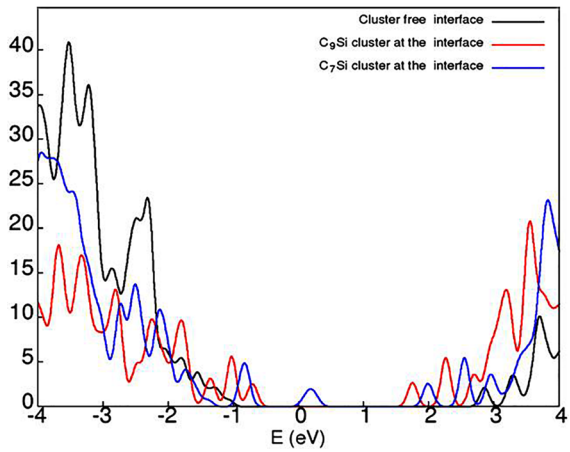

FIG. 3. Computed DOS of SiC/SiO_2 interface structures with different carbon clusters: The interface without any carbon clusters, with 5-atom carbon ring (C7-Si) and 6 carbon ring (C9-Si) clusters. Initially, in the absence of clusters, the energy gap is around 3.1 eV (the marked lines shows the valence band and conduction band edge for the nucleate free interface). New states arise near the valence band edge if carbon clusters are present at the interface. Further details are provided in the supplementary material.

cluster doped SiC or linear carbon clusters at the SiC/SiO_2 interface.[36–39] We compute the DOS for the structural models obtained from our MH-DFT comprising C-Si rings as defect states and compare them with the DOS of pristine SiC. Figure 3 shows defect states emerging in the bandgap of the pristine semiconductor. An atom projected DOS is shown in the same figure, clearly associating these defect levels with the p-states of the carbon clusters in the vicinity of the interface. These results support the assumption that the carbon clusters cause electronic states in the bandgap deteriorating the near-interface mobility.

As our results demonstrate, the thermal oxidation of SiC leads to local, HF etch resistant carbon clusters containing graphitic (sp2) and amorphous (sp3 mixed in sp2) carbon. AFM and Raman spectroscopy together with extensive state-of-the-art atomistic simulations further provide insight into the native SiC oxidation as the root cause for these clusters and their dependence on process parameters and their HF and ozone etching. In particular, our Raman results, along with DFT normal mode analysis, further provide conclusive affirmation of the presence of aromatic and amorphous carbon characteristically different from the carbon contained in the SiC matrix. Further, the DFT calculations also confirm the impact of the defective carbon accumulations on the electronic structure at the interface. In addition to the band structure modification, defects may locally reduce the dielectric breakdown field-strength.

For these reasons, we conclude that the poor performance of the SiC MOS, in comparison to its Si counterparts, is to be attributed to the accumulation of carbon at the interface. The continuous diffusion of C and O during CO/CO_2 release in the thermal oxidation process of SiC modifies the solid matrix, thereby affecting the structural integrity of SiO_2 and the near-interface region of SiC. A wealth of onward work is expected on the basis of our findings to investigate, e.g., (i) the carbon accumulation toward the experimentally observed larger clusters and (ii) the role of passivating agents in such processes.

See the supplementary material for additional results on ozone analysis together with a detailed discussion, along with AFM, Raman, and pDOS data.

The authors acknowledge the financial support from the Swiss National Science Foundation (Projects P300P2-158407, P300P2-174475, and P4P4P2_180669), the Swiss Nanoscience Institute (SNI) (Project No. A10.08 Atolys), and also support from the University of Basel, Paul Scherrer Institute and from ABB Switzerland Ltd. We also acknowledge the CSCS in Lugano (Project Nos. s707 and s752) and the scientific computing core (sciCORE) facility at the University of Basel. This work was partially performed within the NCCR MARVEL. Also, we thank A. Schoener from Ascatron for providing the MOS capacitors and R. Schelldorfer and P. Davenport for their contribution.

REFERENCES

[1]C.-W. Cheng, G. Apostolopoulos, and E. A. Fitzgerald, J. Appl. Phys. **109**(2), 023714 (2011).
[2]J. Brown and G. Moxey, IEEE Electron Device Lett. **10**(10), 71933 (1989).
[3]V. Šimonka, A. Hössinger, J. Weinbub, and S. Selberherr, J. Appl. Phys. **120**(13), 135705 (2016).
[4]V. V. Afanas'ev, F. Ciobanu, G. Pensl, and A. Stesmans, *Silicon Carbide* (Springer, 2004), p. 343.
[5]J. Campi, Y. Shi, Y. Luo, F. Yan, and J. H. Zhao, IEEE Trans. Electron Devices **46**(3), 511 (1999).
[6]E. Pippel, J. Woltersdorf, H. Ö. Ólafsson, and E. Ö. Sveinbjörnsson, J. Appl. Phys. **97**(3), 034302 (2005).
[7]Y. K. Sharma, *New Research on Silicon-Structure, Properties, Technology* (InTech, 2017).
[8]J. R. Williams, G. Y. Chung, C. C. Tin, K. McDonald, D. Farmer, R. K. Chanana, R. A. Weller, S. T. Pantelides, O. W. Holland, and M. K. Das, MRS Online Proc. Libr. **640**, H3.5 (2000).
[9]T. Kimoto and J. A. Cooper, *Fundamentals of Silicon Carbide Technology: Growth, Characterization, Devices and Applications* (John Wiley & Sons, 2014).
[10]T. Christen, A. Ioannidis, and C. Winkelmann, J. Appl. Phys. **117**(8), 084501 (2015).
[11]G. Liu, B. R. Tuttle, and S. Dhar, Appl. Phys. Rev. **2**(2), 021307 (2015).
[12]S. Suzuki, S. Harada, R. Kosugi, J. Senzaki, W.-J. Cho, and K. Fukuda, J. Appl. Phys. **92**(10), 6230 (2002).
[13]K. Shiraishi, *First Principles Study Interfaces Wide Gap Semiconductor*, in Meeting Abstracts, No. 44, pp. 2086–2086 (The Electrochemical Society, 2014), p. 108.
[14]V. V. Afanas'ev, A. Stesmans, and C. I. Harris, Mater. Sci. Forum **264–268**, 857 (1998).
[15]S. Goedecker, W. Hellmann, and T. Lenosky, Phys. Rev. Lett. **95**(5), 055501 (2005).
[16]S. Goedecker, J. Chem. Phys. **120**(21), 9911 (2004).
[17]A. I. Mikhaylov, A. V. Afanasyev, V. V. Luchinin, S. A. Reshanov, A. Schöner, L. Knoll, R. A. Minamisawa, G. Alfieri, and H. Bartolf, Jpn. J. Appl. Phys., Part 1 **55**(8S2), 08PC04 (2016).
[18]Y. Furukawa and K. Nakajima, *Advances in Crystal Growth Research* (Elsevier, 2001).
[19]U. Starke, J. Bernhardt, J. Schardt, and K. Heinz, Surf. Rev. Lett. **6**(6), 1129 (1999).
[20]T. Kimoto, A. Itoh, and H. Matsunami, Phys. Status Solidi B **202**(1), 247 (1997).
[21]J. E. Epler, T. A. Jung, and H. P. Schweizer, Appl. Phys. Lett. **62**(2), 143 (1993).
[22]H. Watanabe and T. Hosoi, in *Physics and Technology of Silicon Carbide Devices* (InTech, 2012).
[23]P. Jamet, S. Dimitrijev, and P. Tanner, J. Appl. Phys. **90**(10), 5058 (2001).
[24]C. I. Harris and V. V. Afanas'ev, Microelectron. Eng. **36**(1–4), 167 (1997).

[25]B. Schaefer, S. Alireza Ghasemi, S. Roy, and S. Goedecker, J. Chem. Phys. **142**(3), 034112 (2015).
[26]B. Aradi, B. Hourahine, and T. Frauenheim, J. Phys. Chem. A **111**(26), 5678 (2007).
[27]E. Rauls, J. Elsner, R. Gutierrez, and Th. Frauenheim, Solid State Commun. **111**(8), 459 (1999).
[28]C. Köhler, Z. Hajnal, P. Deák, T. Frauenheim, and S. Suhai, Phys. Rev. B **64**(8), 085333 (2001).
[29]J. P. Perdew, K. Burke, and M. Ernzerhof, Phys. Rev. Lett. **77**(18), 3865 (1996).
[30]J. Heyd, G. E. Scuseria, and M. Ernzerhof, J. Chem. Phys. **118**(18), 8207 (2003).
[31]M. Syväjärvi, R. Yakimova, and E. Janzén, J. Cryst. Growth **236**(1–3), 297 (2002).
[32]W. Lu, L. C. Feldman, Y. Song, S. Dhar, W. E. Collins, W. C. Mitchel, and J. R. Williams, Appl. Phys. Lett. **85**(16), 3495 (2004).
[33]P. Borowicz, T. Gutt, T. Małachowski, and M. Latek, Diamond Relat. Mater. **20**(5–6), 665 (2011).
[34]M. Makowska-Janusik, A. Kassiba, J. Bouclé, J. F. Bardeau, S. Kodjikian, and A. Désert, J. Phys.: Condens. Matter **17**(33), 5101 (2005).
[35]C. H. Park, B.-H. Cheong, K.-H. Lee, and K. J. Chang, Phys. Rev. B **49**(7), 4485 (1994).
[36]J. M. Knaup, P. Deák, T. Frauenheim, A. Gali, Z. Hajnal, and W. J. Choyke, Phys. Rev. B **72**(11), 115323 (2005).
[37]A. Gavrikov, A. Knizhnik, A. Safonov, A. Scherbinin, A. Bagatur'yants, B. Potapkin, A. Chatterjee, and K. Matocha, J. Appl. Phys. **104**(9), 093508 (2008).
[38]F. Devynck, A. Alkauskas, P. Broqvist, and A. Pasquarello, Phys. Rev. B **83**(19), 195319 (2011).
[39]S. Salemi, N. Goldsman, D. P. Ettisserry, A. Akturk, and A. Lelis, J. Appl. Phys. **113**(5), 053703 (2013).